Title

Parameterization of Acyclic Diaminocarbene Ligands Applied to a Gold(I)-Catalyzed Enantioselective Tandem Rearrangement/Cyclization

Journal

Journal of the American Chemical Society, 139(37)

ISSN

0002-7863

Authors

Niemeyer, Zachary L
Pindi, Suresh
Khrakovsky, Dimitri A
et al.

Publication Date

2017-09-20

DOI

10.1021/jacs.7b08791

Peer reviewed

JACS
JOURNAL OF THE AMERICAN CHEMICAL SOCIETY

Communication

pubs.acs.org/JACS

Parameterization of Acyclic Diaminocarbene Ligands Applied to a Gold(I)-Catalyzed Enantioselective Tandem Rearrangement/Cyclization

Zachary L. Niemeyer,[†] Suresh Pindi,[‡] Dimitri A. Khrakovsky,[‡] Christian N. Kuzniewski,[‡] Cynthia M. Hong,[‡] Leo A. Joyce,[§] Matthew S. Sigman,*[,†] and F. Dean Toste*[,‡]

[†]Department of Chemistry, University of Utah, 315 South 1400 East, Salt Lake City, Utah 84112, United States

[‡]Department of Chemistry, University of California, Berkeley, Berkeley, California 94720, United States

[§]MRL, Department of Process Research & Development, Merck & Co., Inc., Rahway, New Jersey 07065, United States

Supporting Information

ABSTRACT: Computed descriptors for acyclic diaminocarbene ligands are developed in the context of a gold catalyzed enantioselective tandem [3,3]-sigmatropic rearrangement-[2+2]-cyclization. Surrogate structures enable the rapid identification of parameters that reveal mechanistic characteristics. The observed selectivity trends are validated in a robust multivariate analysis facilitating the development of a highly enantioselective process.

The field of homogeneous gold(I) catalysis has experienced remarkable expansion for over a decade, delivering diverse reactivity modes and chemical transformations.[1] This growth has been accompanied by significant advances in enantioselective catalysis using chiral gold complexes.[2] Notwithstanding the pace of these developments, asymmetric catalysis with gold complexes has largely relied on chiral phosphorus based ancillary ligands.[3] Though carbene ligands have been demonstrated to induce differential reactivity in gold catalysis,[4] their utility as chiral ligands has been limited by the lack of modularity and insights into how specific alterations can be leveraged to deliver effective and selective catalysts.[5] These limitations are not unique to gold catalysis, as highly enantioselective transition metal-catalyzed reactions using chiral carbene ligands remain relatively rare compared to their phosphorus-based counterparts.[6]

In this context, the Espinet, Toste, and Slaughter groups have recently identified chiral acyclic diaminocarbene (ADC) ligands as viable architectures to achieve high enantioselectivity (Figure 1).[7] However, the complex interactions that presumably attenuate selectivity are poorly understood, limiting broad application. We therefore chose to interrogate structure-selectivity relationships through the development of novel computed electronic and steric discriptors. The ADC ligand system is well-suited for this analysis as numerous plausible simulated structures can be considered and multiple sites within the molecular framework can be varied. Therefore, the goal of this study was to first develop parameters for the ADC ligand framework, followed by application to the optimization of a gold-catalyzed reaction. The tandem [3,3]-sigmatropic rearrangement-[2+2]-cyclization reaction of propargyl esters provided an attractive reaction for study as an enantioselective process to furnish the highly functionalized products is as yet unreported

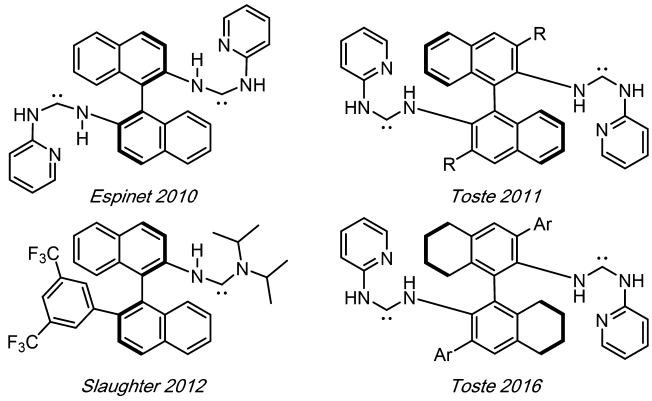

Figure 1. Acyclic diaminocarbene ligands used in gold catalysis.

(Figure 2).[8] Moreover, despite the plethora of gold-catalyzed reactions of propargyl esters, enantioselective transformations employing these reagents remain rare.[9] Herein we report a method to analyze the independent structural features of ADC ligands, allowing the identification of correlative and predictive mathematical models of enantioselectivity. These models provide key insight into why certain catalysts achieve high levels of enantioselectivity and simultaneously provide the foundation to improve asymmetric catalysis.

As noted, the ADC ligand scaffold contains multiple diversification points. As such, we elected to independently probe the H_8-BINAM-aryl groups and the nitrogen heterocycle. The partially hydrogenated backbone was conserved to facilitate synthesis and purification. Previous work from the Toste lab utilizing ADC ligands identified that electronic variation of the 3,3′ aryl groups attenuated the enantioselectivity by as large as 0.6 kcal/mol.[7d] Therefore, electronically diverse 3,5-disubstituted aryl groups were appended to the backbone (aryl groups 1−5, Figure 2), along with additional substitution patterns (aryl groups 5−8, Figure 2). The nitrogen heterocycle was explored primarily using substituted pyridines as other heterocycles proved ineffective (*vide infra*).

Received: August 17, 2017
Published: September 8, 2017

DOI: 10.1021/jacs.7b08791
J. Am. Chem. Soc. 2017, 139, 12943−12946

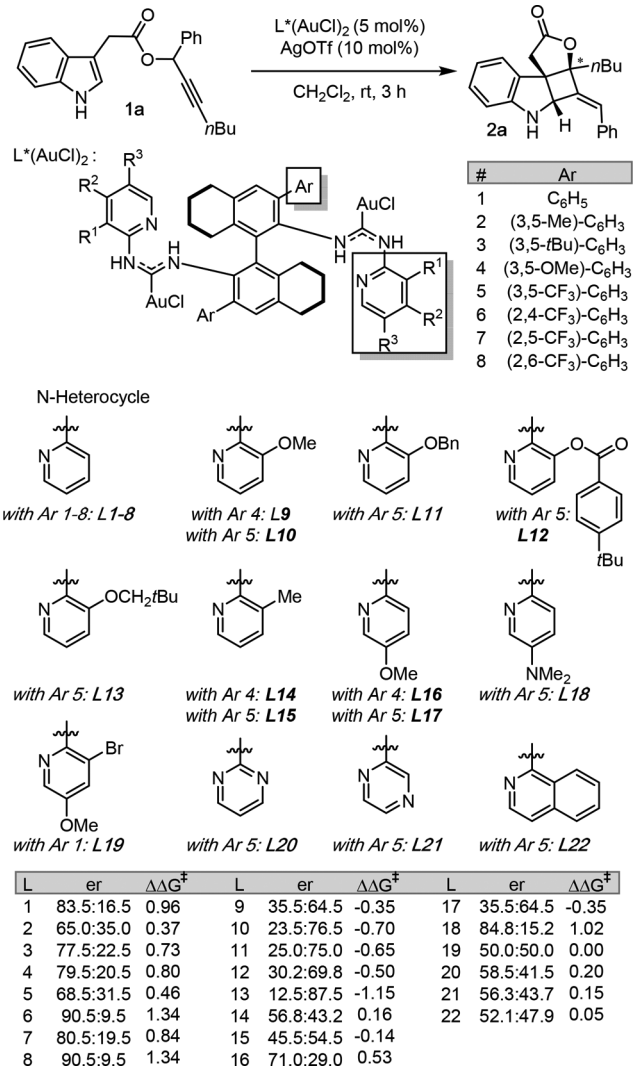

L	er	ΔΔG‡	L	er	ΔΔG‡	L	er	ΔΔG‡
1	83.5:16.5	0.96	9	35.5:64.5	-0.35	17	35.5:64.5	-0.35
2	65.0:35.0	0.37	10	23.5:76.5	-0.70	18	84.8:15.2	1.02
3	77.5:22.5	0.73	11	25.0:75.0	-0.65	19	50.0:50.0	0.00
4	79.5:20.5	0.80	12	30.2:69.8	-0.50	20	58.5:41.5	0.20
5	68.5:31.5	0.46	13	12.5:87.5	-1.15	21	56.3:43.7	0.15
6	90.5:9.5	1.34	14	56.8:43.2	0.16	22	52.1:47.9	0.05
7	80.5:19.5	0.84	15	45.5:54.5	-0.14			
8	90.5:9.5	1.34	16	71.0:29.0	0.53			

Figure 2. Tandem rearrangement-cyclization reaction probed with diverse ligand scaffolds.

Testing an initial training set revealed several notable observations: (1) the enantioselectivity measured for different aryl groups (L1−8) spans a relatively broad range from 90.5:9.5 to 65.0:35.0 ($\Delta\Delta G^{\ddagger}$ = 1.34 to 0.37 kcal/mol) as a function of the substituents, with the best performers containing electron-poor groups; (2) nonpyridine heterocycles perform very poorly (L20−22) suggesting that the pyridine moiety may be privileged in this reaction; (3) the nature of the substituent at the R^1 position of the pyridine has a profound effect. Specifically, the facial selection of the reaction is inverted as a function of placing an oxygen substituent at R^1 in place of hydrogen. These confounding features prompted us to consider treating both diversity elements on the catalyst separately in developing structure enantioselectivity correlations, with an added benefit of considerably lowering the computational load.

In order to simulate and simplify the molecular features of the ADC gold complexes, computational modeling commenced with two surrogate structures as depicted in Figure 3: (1) the aryl group was modeled with the appropriate biaryl carboxylic acid, and (2) the diaminocarbene gold complex was computationally represented by a urea that conserved a hydrogen bond between a terminal urea hydrogen and the nitrogen heterocycle, an initial design element. Ground state geometries were optimized and

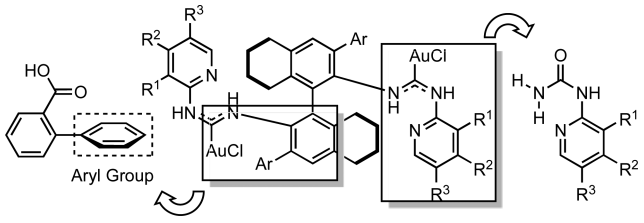

Figure 3. Computed surrogate structures included biaryl carboxylic acids and urea compounds.

diverse parameters were extracted that our teams have found useful in previous multidimensional analyses (see SI for computational details) including simulated charges,[10] IR vibrations and intensities,[11] size measurements,[12] and distances.

Inspecting the data set showcased that the use of nonpyridine heterocyclic ligands (L20−22) lead to nearly racemic products, which prompted us to entertain the possibility that specific structural subclasses may result in distinct mechanistic regimes. Indeed, a univariate plot of $\Delta\Delta G^{\ddagger}$ with the hydrogen bond distance between the terminal urea hydrogen and the heterocycle nitrogen revealed a significant effect on selectivity (Figure 4).

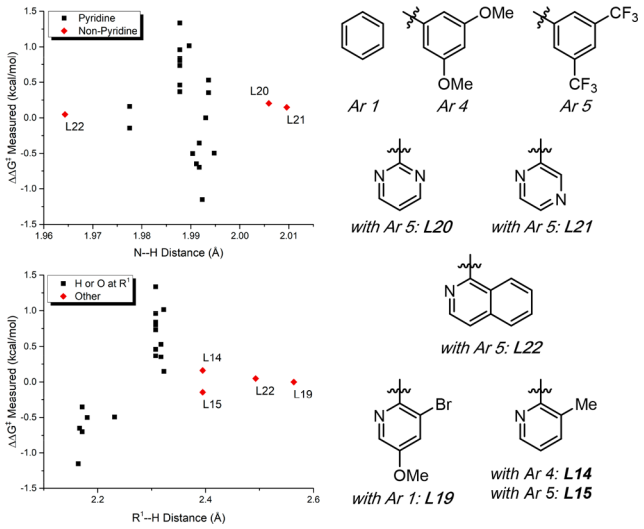

Figure 4. Top: Heterocycles other than pyridine resulted in poor enantioselectivity. Bottom: R^1 substituents have a profound influence on reactivity.

Longer (L20, 21) or shorter (L22) hydrogen bond distances were identified in the nonpyridine heterocycles, underscoring the importance of hydrogen bonding[7a] in these complexes and confirming the disparate selectivity observed using nonpyridine heterocycles.

Having a greater insight into the effect of the heterocycle, we next focused our efforts on the curious observation of inverted selectivity due to oxygen substitution at R^1. Additional parameters were analyzed to specifically probe substitution effects, including bond distances, angles, and size measurements. Most intriguingly, oxygen substitution at R^1 resulted in a slightly distorted sp^2 carbon at C^3 of the arene, wherein the oxygen is directed toward the *ortho* urea structure. This is illustrated by the difference between methoxy and methyl, two similarly sized moieties. The calculated structure with a methoxy substituent at R^1 contains an $R^1{-}C^3{-}C^2$ angle of 115° whereas the methyl substituent is forced away from the urea ($R^1{-}C^3{-}C^2$ angle of 121°). The opposing substitution effects suggest that the oxygen

DOI: 10.1021/jacs.7b08791
J. Am. Chem. Soc. 2017, 139, 12943−12946

atom is attractively interacting with the urea through hydrogen bonding. Indeed, the distance between the R^1 atom and the hydrogen attached to the internal nitrogen of the urea as a function of $\Delta\Delta G^{\ddagger}$ revealed a significant sensitivity (Figure 4). Specifically, hydrogen and oxygen attached to the ring resulted in a clustering of distances whereas other substitutions resulted in longer distances, as expected for a distortion associated with repulsive steric effects.

To confirm the structural distortion that arises from oxygen substitution, a new complex was prepared containing an $-OCH_2$(1-adamantyl) group at R^1 (Figure 6, L23$(AuCl)_2$). Crystal structure analysis (Figure 5) confirmed that the oxygen

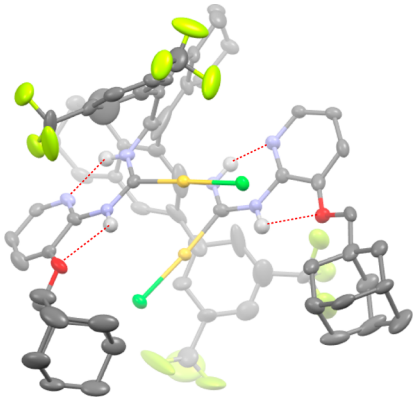

Figure 5. X-ray structure of L23$(AuCl)_2$.

atom is distorted toward the adjacent amine ($R^1-C^3-C^2 = 115°$) in excellent agreement with the computed structures ($R^1-C^3-C^2 = 115°$). This result indicates that the urea surrogate structures are accurately portraying the gold complexes, inspiring confidence in the previously identified trends.

As a function of the clustering analyses performed above, six complexes were identified as potential outliers (14, 15, 19–22). These catalysts were removed from further consideration as they are likely functioning in a mechanistically distinct manner. The remaining 16 complexes were used as a training set for multivariate linear regression modeling (Figure 6). Six additional pyridine structures retaining either H or O at R^1 were utilized as an internal validation set (L23–28). A relatively simple statistical model was obtained containing only two parameters to describe this complex system: the NBO charge of the carbonyl carbon in the biaryl carboxylic acid and the distance between the R^1 substituent and the hydrogen attached to the internal nitrogen of the urea. One final external validation complex (L29) confirmed the robustness of the identified model. In sum, the predicted versus measured values are in excellent agreement with an R^2 of 0.90 and an average error of 0.21 kcal/mol.

The simplicity of this model allows for facile interpretation. As depicted in Figure 4, hydrogen or oxygen substitution largely influences the R^1-H distance, with each atom clustering. The binary effect of this change is the cause for the bifurcation of enantioselectivity, with opposite enantiomers of product formed despite the (*S*) enantiomer of the H-binaphthyl backbone being maintained in all complexes. Thus, the through-space and inductive effects from the aryl group primarily influence the degree of enantioselectivity, represented by NBO_C. Catalysts that lead to enhanced enantioselectivity contain 2-substituted aryl groups (aryl **6**–**8**), which influence the dihedral angle between the arene and backbone (simulated aryl–aryl dihedral = 80–88°). Accordingly, the most electron-withdrawing aryl group,

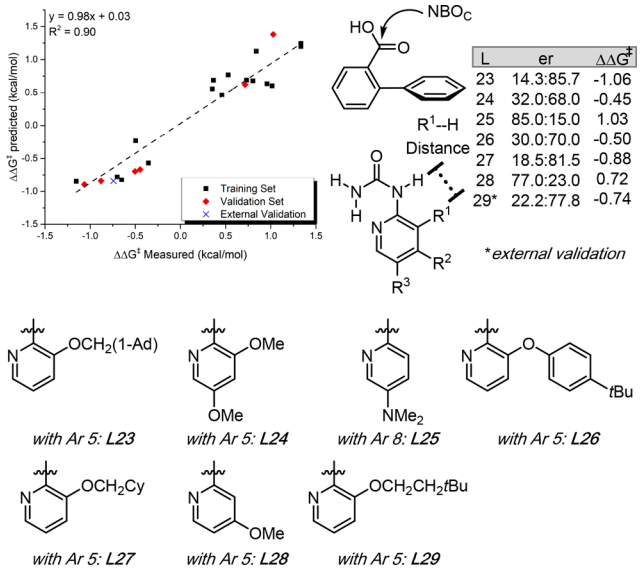

Figure 6. Simple model utilizing two descriptors provides excellent ability to predict reaction outcomes.

2,6-$(CF_3)_2C_6H_3$, results in a relatively positively charged carbon (NBO_C = 0.788), and complex **8** affords the highest enantioselectivity when used (90.5:9.5). Interestingly, the biaryl carboxylic acid correctly reproduces the differential effects of 2,6-bis(trifluoromethyl) aryl substitution versus 3,5-bis(trifluoromethyl). In essence, use of 3,5-$(CF_3)_2C_6H_3$ as an aryl group results in lower enantioselectivities (more negative), and NBO_C accurately depicts a less positive charge (0.777), a consequence of the aryl–aryl ring dihedral and the aryl–carboxylic acid dihedral. Among aryl groups **1**–**5**, which contain a similar aryl–aryl dihedral (range = 50–55°), the simulated structure for 3,5-CF_3 contains the most overlap between the carboxylic acid and the aryl ring (dihedral = 20° versus 27–31°) resulting in a less positively charged carbon. The ability to accurately describe the nuanced electronic interactions with the metal center influencing selectivity highlights the utility of the simulated structures.

Pleased by the robust mathematical model that offers a simple interpretation, we returned to optimizing the rearrangement-cyclization under study. The importance of through space interactions allowed us to hypothesize that a more nonpolar solvent would increase reaction enantioselectivity. Indeed, swapping methylene chloride for toluene increased both the enantiomeric excess and yield. Evaluation of a modest array of substrates revealed the utility of this reaction as well as limitations (Figure 7). Bulkier alkyl groups at R″ resulted in higher enantiodiscrimination using L23; however, an opposite effect was observed with L18. Indeed, better yields and enantioselectivities were observed with L23 than with L18. Various electron withdrawing and donating substituents were tolerated on the indole ring at C5 and C6. However, substitution at C4 of the indole ring resulted in nearly racemic products.

In summary, a gold catalyzed tandem [3,3]-sigmatropic rearrangement-[2+2]-cyclization has been explored and utilized as a platform to interrogate acyclic diaminocarbene ligands. Through computational modeling of surrogate structures, parameters to describe this developing ligand class have been introduced. These factors were combined with reaction enantioselectivities to interrogate structural details, allowing for the identification of an unexpected hydrogen bond. Further

DOI: 10.1021/jacs.7b08791
J. Am. Chem. Soc. 2017, 139, 12943–12946

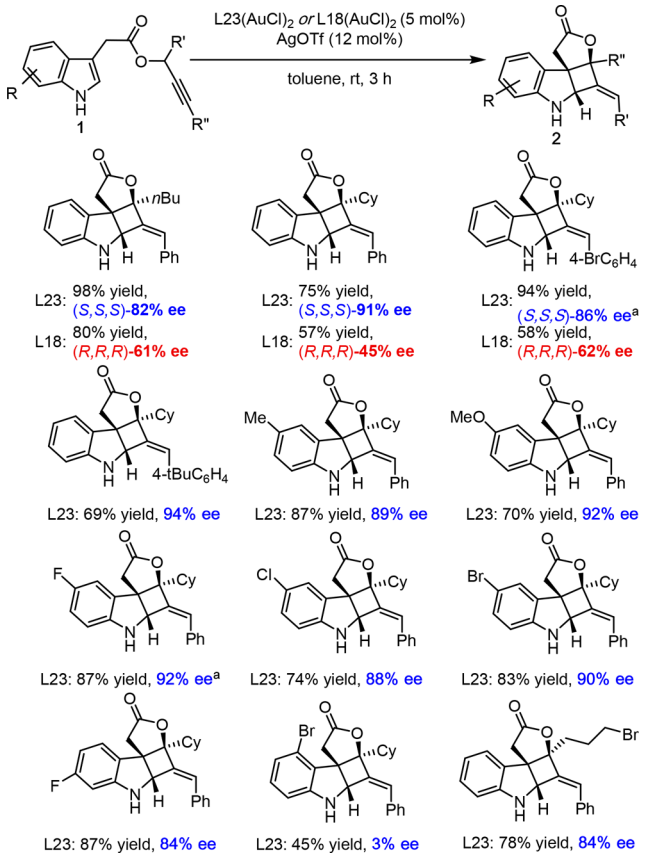

Figure 7. Tandem [3,3]-sigmatropic rearrangement-[2+2]-cyclization reaction scope. Unless otherwise noted, all reactions were carried out with 1 (0.05 mmol) in toluene (1.0 mL) for 3 h. Yields are determined by NMR spectroscopy. ee was determined by chiral HPLC analysis and are averages from two runs. [a]Absolute configuration assigned by VCD (see Supporting Information).

application of this ligand class and the described parameters is underway.

■ ASSOCIATED CONTENT

Supporting Information

The Supporting Information is available free of charge on the ACS Publications website at DOI: 10.1021/jacs.7b08791.

Data for $C_{70}H_{68}Au_2Cl_2F_{12}N_6O_2$ (CIF)

Experimental procedures, additional reaction optimization, and characterization data (PDF)

■ AUTHOR INFORMATION

Corresponding Authors

*sigman@chem.utah.edu

*fdtoste@berkeley.edu

ORCID

Matthew S. Sigman: 0000-0002-5746-8830

F. Dean Toste: 0000-0001-8018-2198

Notes

The authors declare no competing financial interest.

■ ACKNOWLEDGMENTS

F.D.T. gratefully acknowledges NIGMS (R35 GM118190) and M.S.S. thanks the NSF (CHE-1361296) for financial support of this work. C.N.K. thanks the Swiss National Science Foundation (SNF) for a postdoctoral fellowship. The support and resources from the Center for High Performance Computing at the University of Utah are gratefully acknowledged.

■ REFERENCES

(1) (a) Dorel, R.; Echavarren, A. M. *Chem. Rev.* **2015**, *115*, 9028−9072. (b) Joost, M.; Amgoune, A.; Bourissou, D. *Angew. Chem., Int. Ed.* **2015**, *54*, 15022−15045. (c) Pflasterer, D.; Hashmi, A. S. K. *Chem. Soc. Rev.* **2016**, *45*, 1331−1367. (d) Miro, J.; del Pozo, C. *Chem. Rev.* **2016**, *116*, 11924−11966. (e) Wei, Y.; Shi, M. *ACS Catal.* **2016**, *6*, 2515−2524.

(2) (a) Pradal, A.; Toullec, P. Y.; Michelet, V. *Synthesis* **2011**, *2011*, 1501−1514. (b) Wang, Y.-M.; Lackner, A. D.; Toste, F. D. *Acc. Chem. Res.* **2014**, *47*, 889−901. (c) Zi, W.; Toste, F. D. *Chem. Soc. Rev.* **2016**, *45*, 4567−4589. (d) Li, Y.; Li, W.; Zhang, J. *Chem. - Eur. J.* **2017**, *23*, 467−512.

(3) (a) Teller, H.; Flügge, S.; Goddard, R.; Fürstner, A. *Angew. Chem., Int. Ed.* **2010**, *49*, 1949−1953. (b) González, A. Z.; Benitez, D.; Tkatchouk, E.; Goddard, W. A.; Toste, F. D. *J. Am. Chem. Soc.* **2011**, *133*, 5500−5507. (c) Wang, W.; Hammond, G. B.; Xu, B. *J. Am. Chem. Soc.* **2012**, *134*, 5697. (d) Wang, Y.; Wang, Z.; Li, Y.; Wu, G.; Cao, Z.; Zhang, L. *Nat. Commun.* **2014**, *5*, 3470. (e) Christian, A. H.; Niemeyer, Z. L.; Sigman, M. S.; Toste, F. D. *ACS Catal.* **2017**, *7*, 3973−3978.

(4) (a) Marion, N.; Nolan, S. P. *Chem. Soc. Rev.* **2008**, *37*, 1776−1782. (b) Gorin, D. J.; Sherry, B. D.; Toste, F. D. *Chem. Rev.* **2008**, *108*, 3351−3378. (c) Klahn, P.; Kirsch, S. F. *ChemCatChem* **2011**, *3*, 649−652.

(5) (a) Diez-González, S.; Nolan, S. P. *Coord. Chem. Rev.* **2007**, *251*, 874−883. (b) Gusev, D. G. *Organometallics* **2009**, *28*, 6458−6461. (c) Dröge, T.; Glorius, F. *Angew. Chem., Int. Ed.* **2010**, *49*, 6940−6952.

(6) (a) César, V.; Bellemin-Laponnaz, S.; Gade, L. H. *Chem. Soc. Rev.* **2004**, *33*, 619−636. (b) Wu, L.; Salvador, A.; Dorta, R. Chiral Monodendate N-Heterocyclic Carbene Ligands in Asymmetric Catalysis. In *N-Heterocyclic Carbenes: Effective Tools for Organometallic Synthesis*; Nolan, S. P., Ed.; Wiley-VCH Verlag GmbH & Co. KGaA: Weinheim, Germany, 2014. (c) Janssen-Müller, D.; Schlepphorst, C.; Glorius, F. *Chem. Soc. Rev.* **2017**, *46*, 4845−4854.

(7) (a) Bartolomé, C.; García-Cuadrado, D.; Ramiro, Z.; Espinet, P. *Inorg. Chem.* **2010**, *49*, 9758−9764. (b) Wang, Y.-M.; Kuzniewski, C. N.; Rauniyar, V.; Hoong, C.; Toste, F. D. *J. Am. Chem. Soc.* **2011**, *133*, 12972−12975. (c) Handa, S.; Slaughter, L. M. *Angew. Chem., Int. Ed.* **2012**, *51*, 2912−2915. (d) Khrakovsky, D. A.; Tao, C.; Johnson, M. W.; Thornbury, R. T.; Shevick, S. L.; Toste, F. D. *Angew. Chem., Int. Ed.* **2016**, *50*, 906−910. See also: (e) Francos, J.; Grande-Carmona, F.; Faustino, H.; Iglesias-Sigüenza, J.; Diez, E.; Alonso, I.; Fernández, J. M.; López, F.; Mascareñas, J. L.; Lassaletta, J. M. *J. Am. Chem. Soc.* **2012**, *134*, 14322−14325.

(8) Zhang, L. *J. Am. Chem. Soc.* **2005**, *127*, 16804−16805.

(9) For a general reviews of propargyl esters in gold catalysis, see: (a) Marion, N.; Nolan, S. P. *Angew. Chem., Int. Ed.* **2007**, *46*, 2750−2752. (b) Wang, S.; Zhang, G.; Zhang, L. *Synlett* **2010**, *2010*, 692−706. For examples of phosphinegold(I)-catalzyed reactions of enantioselective reactions of propargyl esters, see: (c) Pirovano, V.; Arpini, E.; Dell'Acuqa, M.; Vicente, R.; Abbiati, G.; Rossi, E. *Adv. Synth. Catal.* **2016**, *358*, 403−409. (d) Garayalde, D.; Krüger, K.; Nevado, C. *Angew. Chem.* **2011**, *123*, 941−945. (e) Watson, I. D. G.; Ritter, S.; Toste, F. D. *J. Am. Chem. Soc.* **2009**, *131*, 2056−2057. (f) Johansson, M. J.; Gorin, D. J.; Staben, S. T.; Toste, F. D. *J. Am. Chem. Soc.* **2005**, *127*, 18002−18003.

(10) (a) Santiago, C. B.; Milo, A.; Sigman, M. S. *J. Am. Chem. Soc.* **2016**, *138*, 13424−13430. (b) Glendening, E. D.; Landis, C. R.; Weinhold, F. *J. Comput. Chem.* **2013**, *34*, 1429−1437.

(11) (a) Milo, A.; Bess, E. N.; Sigman, M. S. *Nature* **2014**, *507*, 210−214. (b) Bess, E. N.; Guptill, D. M.; Davies, H. M. L.; Sigman, M. S. *Chem. Sci.* **2015**, *6*, 3057−3062. (c) Milo, A.; Neel, A. J.; Toste, F. D.; Sigman, M. S. *Science* **2015**, *347*, 737−743. (d) Niemeyer, Z. L.; Milo, A.; Hickey, D. P.; Sigman, M. S. *Nat. Chem.* **2016**, *8*, 610−617.

(12) (a) Harper, K. C.; Sigman, M. S. *Science* **2011**, *333*, 1875−1878. (b) Harper, K. C.; Bess, E. N.; Sigman, M. S. *Nat. Chem.* **2012**, *4*, 366−374.